

N. NILIUS^{✉,*}
T.M. WALLIS^{**}
W. HO

Tailoring electronic properties of atomic chains assembled by STM

Department of Physics and Astronomy and Department of Chemistry, University of California, Irvine, CA 92697-4575, USA

Received: 9 March 2004/Accepted: 22 October 2004

Published online: 23 February 2005 • © Springer-Verlag 2005

ABSTRACT Atomic chains were assembled from single Au and Pd atoms on a NiAl(110) surface, using the tip of a scanning tunneling microscope. The electronic properties of the chains were investigated by spatially resolved conductance spectroscopy and microscopy, revealing the development of a one-dimensional, free-electron-like band. Onset energy, effective electron mass, and spatial localization of the band were influenced by structural and chemical modifications of the chains. The experiments demonstrate the effects of interatomic spacing and elemental composition of the chains, as well as the roll of local impurities and adsorption on the properties of the one-dimensional electronic system.

PACS 68.37.Ef; 73.21.Fg; 73.22.-f; 68.43.-h

1 Introduction

The exceptional properties of one-dimensional (1D) systems have initiated a large number of experimental and theoretical investigations in recent years. Spatial confinement perpendicular to the system axis induces pronounced discretization of electronic states [1–3]. In systems with finite length, size effects also occur along the axis, leading to quantized electron transport. The strong electron–electron correlation in one dimension is known to induce metal–insulator (Mott) transitions [4]. The enhanced electron–phonon coupling favors static rearrangements of the atom positions, driven by the formation of new zone boundaries in reciprocal space (Peierls distortion) [5]. Low-dimensional electronic systems also exhibit a reduced screening efficiency, which leads to anomalously long interaction lengths [6]. The reduction to one spatial dimension facilitates the general understanding of the interplay between structural and electronic properties of matter.

One-dimensional systems are not only of scientific interest. The unbroken trend in miniaturization of electronic devices pushes the structure size from the classical into the

quantum-mechanical regime. Nanowires have a great potential as future gas sensors due to their favorable surface-to-volume ratio [7, 8]. Low-dimensional systems also play a decisive role in heterogeneous catalysis. Several approaches have been successfully implemented to manufacture 1D structures. Metal deposition on vicinal surfaces leads to decoration of step edges and formation of nanowires [8–10]. Adsorption on template surfaces with a well-defined geometry stimulates directional growth [11]. For specific substrate–adsorbate systems, a self-assembly of 1D structures has been observed, driven by the minimization of surface free energy and stress relief [12–15]. On a larger scale, lithographic techniques are available to produce linear structures.

The methods mentioned above allow the preparation of 1D systems on extended surface areas. However, statistical disorder, defects, and imperfections cannot be avoided in the preparation process. Neither the exact length of the wires nor the position and type of atoms in the structure can be controlled. Atom manipulation with the tip of a scanning tunneling microscope (STM) enables the assembly of linear aggregates with atomic precision [16–18]. Using the imaging and spectroscopic modes of this technique, the structures can directly be investigated on the atomic scale. The potential of preparing and analyzing nanostructures within the STM has been demonstrated in a number of experiments, describing the confinement of surface states in artificial quantum corals [19], the assembly of Cr trimers with distinct magnetic properties [20], and the formation of single carbonyls by tip-induced chemical reactions [21].

This paper describes a series of STM experiments, which focus on the fabrication and analysis of atomic chains assembled from single atoms on a NiAl(110) surface. The chain formation induces the development of a 1D electron band, originating from a single resonance state in individual atoms. Several methods were adapted to modify the band properties, such as changes of length, lattice constant, and elemental composition of the chains. The influence of local impurities and molecular adsorption on the properties of the 1D electronic system was also examined.

2 Experiment

The measurements were performed in an ultra-high-vacuum STM operating at 12 K [22]. STM tips were electrochemically etched from polycrystalline W wire and

✉ Fax: +49-30-8413-4101, E-mail: nilius@fhi-berlin.mpg.de

*Present address: Fritz-Haber-Institut der MPG, Faradayweg 4–6, 14195 Berlin, Germany

**Present address: National Institute of Standards and Technology, Boulder, CO 80305, USA

prepared in situ by self-sputtering and annealing. The microscopic tip structure was optimized by controlled crashes into the sample surface until circular topographic images and Gaussian-shaped conductance peaks could be obtained for single adatoms. The NiAl(110) surface was prepared by alternate cycles of Ne⁺ sputtering and annealing to 1300 K. Pd and Au atoms were evaporated from two resistively heated crucibles and deposited onto the surface at 12 K. The single atoms preferentially adsorb on Ni–Ni bridge sites. The operation of the STM could be switched between imaging and manipulation modes by changing the tunneling parameters. An attractive tip–adsorbate interaction at voltages below 5 mV and tunneling currents above 10 nA induce a controlled motion of single adatoms across the surface. The atom jumps from binding site to binding site while it follows the trajectory of the tip. Manipulation of Pd atoms requires a smaller tunneling resistance (V/I) compared to Au atoms, which indicates a larger Pd–NiAl interaction. The controlled displacement of single atoms was employed to construct linear chains with a well-defined orientation, length, and composition. Operating the STM at larger sample bias ($V \geq 0.1$ V) and reduced current ($I \leq 1.0$ nA) allowed imaging and analysis of the chains. The local electronic structure of the sample surface was determined by conductance spectroscopy, detecting the first derivative of the tunneling current as a function of sample bias (dI/dV) with a lock-in amplifier. The dI/dV signal provides a measure of the local density of states (LDOS) at the position of the tip.

3 Gold chains on NiAl(110)

Chains of single Au atoms have been assembled along the [001] direction of NiAl(110), using the Ni troughs as a natural template (Fig. 1a) [23]. The lattice constant of the chains is given by the distance between two Ni–Ni bridge sites of 2.89 Å. Measured chain lengths are always 3–5 Å larger than computed ones due to the electronic cloud centered on single atoms. The chain formation is accompanied by characteristic changes in the electronic structure (Fig. 1b). The dI/dV spectrum of a single Au atom is dominated by a resonance at 1.95 V, originating from a hybridization of the Au 6*sp* level and the NiAl *sp* band [24]. The state lies in a pseudo-gap of the NiAl bulk bands above the Fermi level and has a spatial extension comparable to the apparent size of the atom in STM images. A splitting of the resonance into two peaks at 1.45 and 2.25 V is observed for Au dimers. The peak splitting results from direct and substrate-mediated coupling between the Au-induced electronic states and scales with the inverse atom–atom separation [24]. In Au trimers, a third dI/dV peak appears in the spectra. Further increase in chain length causes a gradual shift of the low-energy resonance toward the Fermi level, from 1.1 V in Au₃, 0.95 V in Au₄, 0.85 V in Au₅, and to 0.75 V in a 20-atom chain. The energy position of this peak decreases proportionally to the squared reciprocal chain length ($E_1 \sim L^{-2}$), reflecting the general behavior of electronic states in a 1D quantum well [25].

Spatially resolved conductance measurements on Au chains reveal a distinct oscillatory behavior in the dI/dV signal along the chain axis [23, 26]. The modulations were observed in dI/dV images, mapping the conductance at a se-

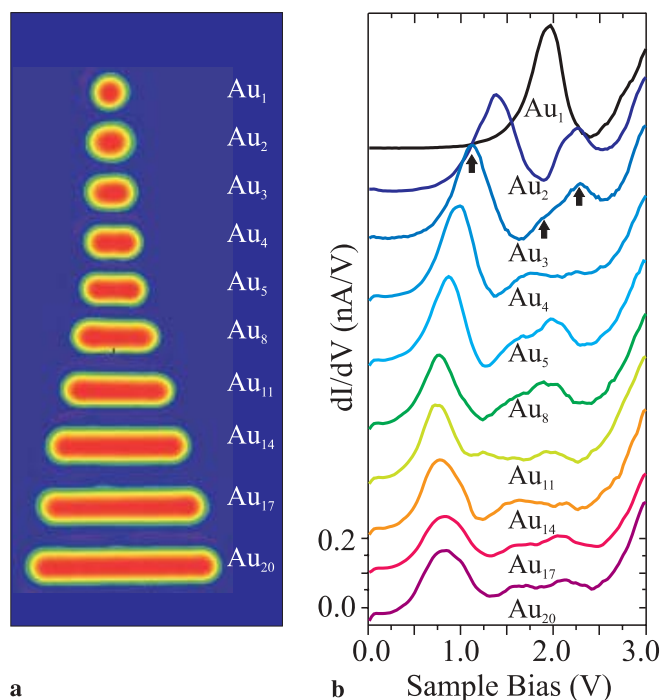


FIGURE 1 **a** STM topographic images and **b** dI/dV spectra of a Au monomer and Au chains of different lengths on NiAl(110). The spectra were taken in the center of the chain with $V_{\text{sample}} = 3.0$ V and $I = 1.0$ nA. The resonance state of the Au monomer at 1.95 V splits into a doublet in the dimer, a triplet in the trimer, and develops into a 1D electronic band as the chain length increases to 20 Au atoms. The three dI/dV peaks of the Au trimer are marked with *arrows*

lected bias voltage (Fig. 2a), as well as in spectral series taken along the chain. The oscillations reflect standing wave patterns of the electron density in the quantum well, whereby the number of maxima and minima along the chain increases with the applied sample bias. Particularly well-resolved wave patterns were obtained when the sample bias matches an eigenstate E_n of the system [25]. The dI/dV maps of the Au₁₁ chain shown in Fig. 2a were taken at voltages corresponding to the 2nd, 3rd, 4th, and 5th eigenstates and clearly show the appearance of one, two, three, and four nodes in the dI/dV signal. The energy position of eigenstates E_n in the quantum well was exactly determined by fitting the experimental dI/dV oscillations to a 1D ‘particle-in-a-box’ model [23, 27]. The obtained relationship between E_n and the wave number $k_n = n\pi/L$ of the charge-density oscillations corresponds to the theoretical dispersion in a 1D quantum well with infinite walls [28]:

$$E_n = E_0 + \frac{\hbar^2}{2m_{\text{eff}}} k_n^2.$$

The effective mass m_{eff} of electronic states in the Au₁₁ chain was determined to be 50% of the free-electron mass m_e . Similar values were obtained for Au chains containing up to 20 atoms.

4 Structural modifications of atomic chains

The twofold symmetry of the NiAl(110) surface supports the construction of two kinds of chains. Along the

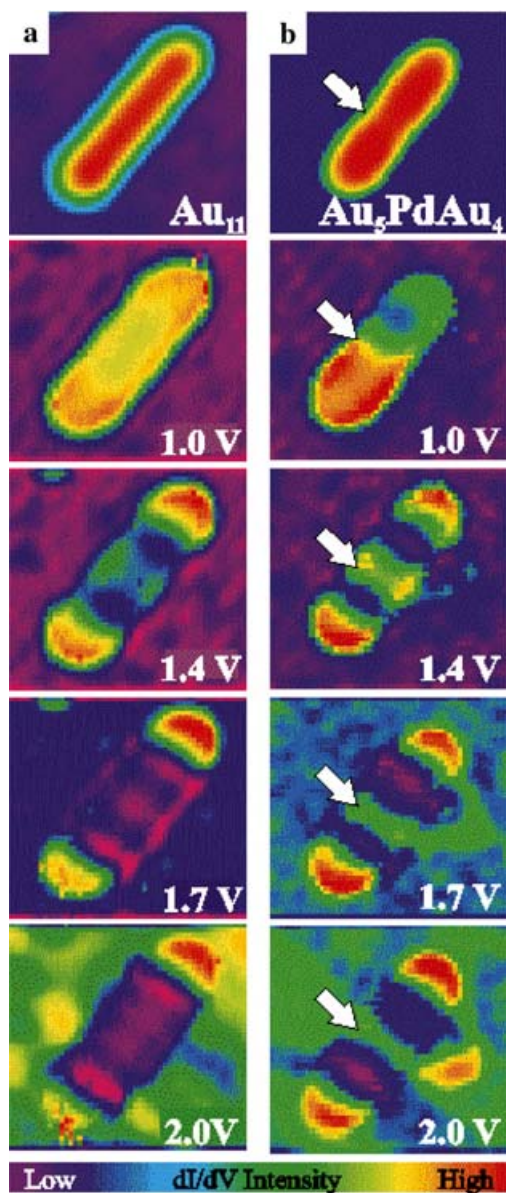


FIGURE 2 Topographic (top) and dI/dV images of **a** Au_{11} and **b** Au_5PdAu_4 on $\text{NiAl}(110)$ taken at $I = 1.0$ nA and the indicated bias voltages. The selected bias values match the energy positions of eigenstates in the bare Au_{11} chain. The dI/dV images show standing wave patterns corresponding to the 2nd, 3rd, 4th, and 5th quantum-well states. Due to the Pd impurity (marked with an arrow), the electronic states in **(b)** become localized on both chain sections separated by the Pd atom

[001] direction, neighboring Au adsorption sites are separated by 2.89 \AA (Fig. 3a). The properties of Au chains with this orientation were discussed above (Figs. 1 and 2a). Along $[1\bar{1}0]$, the distance between adjacent binding sites is increased to 4.08 \AA . An STM topographic image of a $[1\bar{1}0]$ -oriented Au_{11} chain is presented in Fig. 3b. Conductance spectra of Au chains with both orientations reveal distinct differences in their electronic structure (Fig. 3c) [29]. Spectra of the [001] chain are dominated by a broad resonance at 0.75 V , reflecting the onset of quantum-well states. The corresponding peak for the $[1\bar{1}0]$ chain is blue shifted to 1.50 V and has a smaller intrinsic width. The dI/dV peak results from the overlap of the first three quantum-well states in the chain, which are very

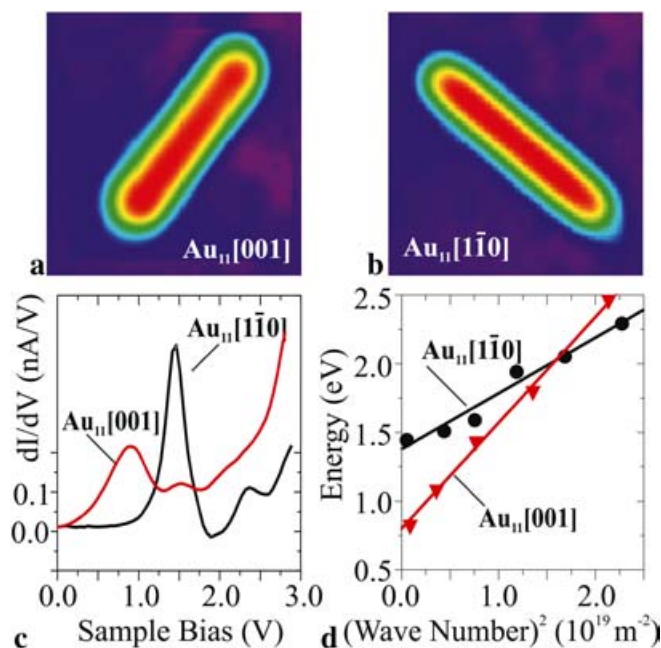


FIGURE 3 STM topographic images of Au_{11} chains constructed along **a** the [001] and **b** the $[1\bar{1}0]$ directions of $\text{NiAl}(110)$. **c** dI/dV spectra taken in the center of both chains. **d** Energy levels of Au_{11} [001] and Au_{11} $[1\bar{1}0]$ chains plotted as a function of squared wave number $k = n\pi/L$, where L is the chain length. Level positions were determined from spatially resolved dI/dV measurements along the chain axis, showing standing wave patterns according to the quantum number n of the quantum-well states. The straight lines represent fits of the energy levels to a 1D ‘particle-in-a-box’ model, yielding an effective electron mass of $1.0m_e$ for Au_{11} $[1\bar{1}0]$ and $0.5m_e$ for Au_{11} [001]. The differences in electronic properties are due to the larger atom–atom separation in Au_{11} $[1\bar{1}0]$ (4.08 \AA) compared to Au_{11} [001] (2.89 \AA)

close in energy. The electron-density waves associated with these levels strongly interfere and standing wave patterns are hardly resolved at the onset of the $[1\bar{1}0]$ band. The 4th eigenstate in the quantum well is detected at 1.65 V , and the 5th and 6th states at 1.9 and 2.1 V , respectively. The small energy separation of electronic states points to a reduced dispersion of the band formed in the $[1\bar{1}0]$ chain. A complete analysis of the spectroscopic data yields an effective electron mass of $1.0m_e$, which is two times larger than for the band in the Au_{11} [001] chain (Fig. 3d). The difference results from an increased atom–atom separation in the $[1\bar{1}0]$ direction, causing smaller overlap and inefficient hybridization between neighboring orbitals in the chain. A similar trend in coupling strength was already observed for Au dimers assembled in both directions [24]. Whereas the [001] dimer shows an energy splitting of 0.8 V between low- and high-energy states, the separation decreases to 0.6 V for the $[1\bar{1}0]$ dimer.

5 Influence of elemental composition on the chain electronic properties

A second means to modify the 1D electronic structure of atomic chains is an alteration of their elemental composition. To examine the influence of different atomic species on the band-formation process, Pd and Au atoms were co-adsorbed on the NiAl surface (Fig. 4a). The two elements were chosen because of the different electronic configuration

of the isolated atoms. A free Au atom has a half-filled $6s$ orbital, whereas the corresponding Pd $5s$ orbital is unfilled and the highest occupied orbital has d character. Pd and Au atoms on the NiAl(110) surface can be distinguished already from STM topographic images. At +2.0 V sample bias, the Au atoms appear with a larger apparent height than the Pd atoms. The difference diminishes in images taken at higher or lower voltages. This bias-dependent height contrast originates from the presence of single-atom resonances with different energies in Au_1 and Pd_1 , as derived from dI/dV spectroscopy (Fig. 4b). Single Au atoms show the above-mentioned resonance level at 1.95 V, which shifts to 2.80 V in Pd atoms [30]. The shift is the consequence of the missing electron in the Pd $5s$ orbital, which alters the hybridization mechanism with the NiAl sp band.

The assembly of [001] atomic chains from single Pd atoms leads to a development of quantum-well states, similar to those observed in Au chains (Fig. 4c) [31]. The onset energy is considerably blue shifted from 0.75 V for Au_{11} to 1.51 V for Pd_{11} (Fig. 4d). The electron levels in the Pd quantum well were identified according to their quantum number by imaging the standing wave patterns as a function of sample bias. Also, for Pd chains on NiAl(110), a parabolic dependence of the level energy on the quantum number n and the inverse

chain length L was found, confirming the one-dimensional character of the system [25]. The dispersion of the Pd electronic states corresponds to an effective mass of $0.65m_e$ [31]. The smaller curvature and reduced electron mobility of the Pd-induced band are attributed to a stronger spatial confinement of the initial Pd $5s$ orbital compared to the Au $6s$ orbital, which reduces the overlap between neighboring electronic states in the chain. Furthermore, the next-neighbor distance in bulk Pd of 2.75 Å is much shorter than the Ni–Ni distance of 2.89 Å.

The alloying of Au and Pd on the atomic scale was studied by constructing chains with alternating atomic species [31]. In contrast to the respective monomers on the NiAl(110) surface, Au and Pd atoms become indistinguishable in mixed atomic chains (Fig. 4c). The vanishing difference in apparent height clearly indicates strong hybridization between Au- and Pd-induced electronic states. Conductance spectroscopy on $Au(PdAu)_5$ reveals indeed the development of delocalized quantum-well states, manifested by the observation of standing wave patterns along the chain axis. The low-energy dI/dV resonance in alloy chains was observed at 1.0 V, compared to 0.75 V in Au_{11} and 1.51 V in Pd_{11} chains (Fig. 4d). Also, the effective mass describing the dispersion of electronic states in $Au(PdAu)_5$ ($0.56m_e$) is located in between the values obtained for pure Au and Pd chains, demonstrating the effective electronic coupling between both species.

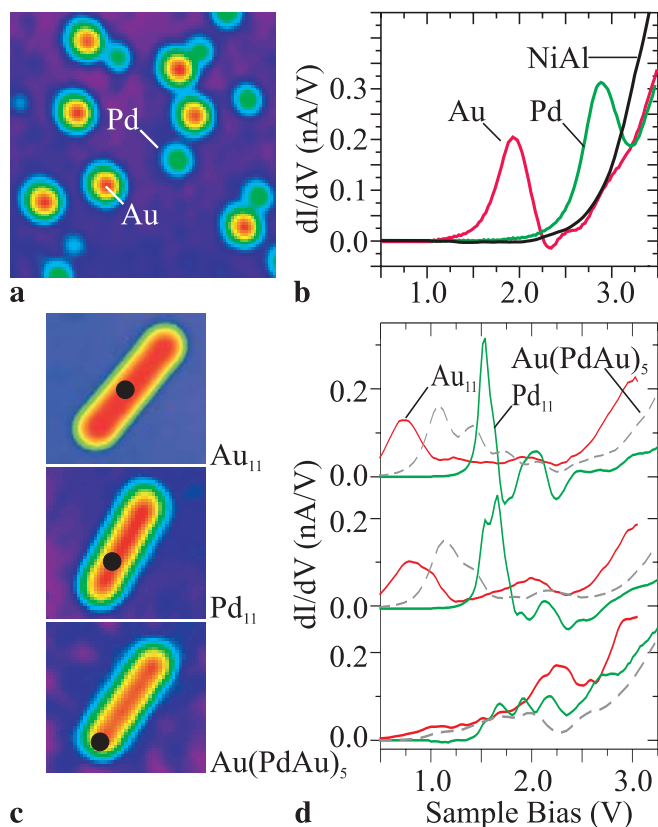


FIGURE 4 **a** Topographic STM image and **b** dI/dV spectra of single Au and Pd atoms on NiAl(110). The image size is 80×80 Å; the gap was set with $V_{\text{sample}} = 2.0$ V and $I = 1.0$ nA. **c** STM topographic images and **d** dI/dV spectra of Au_{11} , Pd_{11} , and $Au(PdAu)_5$ chains on NiAl(110). The spectra were taken in the center (*upper curves*), the lower half (*middle curves*), and at the end (*lower curves*) of the three chains. The tip positions for spectroscopy are denoted by *dots* in (c). The shift in the onset of the 1D band from 0.75 V in Au_{11} to 1.0 V in $Au(PdAu)_5$ and 1.5 V in Pd_{11} is apparent

6 Local impurities in atomic chains

Although strong hybridization of Au and Pd orbitals has been observed in alloy chains with regular alternation of the two species, a completely different picture arises when single Pd atoms are dispersed in a Au chain. Two different impurity structures were synthesized and examined on the NiAl surface, a Au_9 chain with a Pd monomer and a Pd dimer embedded in the center [30]. Conductance maps of Au_5PdAu_4 show no standing wave patterns extending along the entire chain axis, but dI/dV oscillations confined to both Au subchains (Fig. 2b). The electronic properties of the two chain sections separated by the Pd impurity were analyzed by dI/dV spectroscopy and found to be similar to those of isolated Au chains with the same number of atoms. At the position of the Pd impurity, no characteristic quantum-well states are resolved and dI/dV spectra show only a resonance state at 2.1 V. Apparently, the presence of a single Pd atom in Au chains leads to the disruption of the 1D electronic system. Delocalized quantum-well states become confined to the two Au chain sections and localized energy levels develop at the position of the Pd impurity [30]. For a single Pd atom in Au chains, this impurity level lies at 2.1 V and does not shift in energy when additional Au atoms are attached to both sides of the chain. The level is clearly red shifted with respect to the 2.8-V resonance in isolated Pd atoms, reflecting the reduced electron potential in the neighborhood of the Au atoms in the chain. The Pd dimer embedded in a Au_9 chain shows a dI/dV doublet with peaks at 2.25 and 2.95 V. In contrast to the Pd_1 impurity level, the energy positions of the split states are only weakly red shifted from the positions in isolated Pd dimers.

7 Molecular adsorption on atomic chains

Strong modifications in the electronic structure can also be triggered by CO adsorption on artificial chains on the NiAl surface. The binding of CO to Au monomers can readily be followed in STM topographic images taken before and after gas exposure. In images taken at +2.0 V sample bias, Au atoms with an adsorbed CO molecule exhibit a strongly reduced apparent height compared to bare atoms [32]. At low sample bias, the gold carbonyls (AuCO) are imaged slightly brighter than bare Au atoms. Conductance spectroscopy reveals the origin of this contrast reversal. The tunneling efficiency into Au monomers is determined by the single-atom resonance at +1.95 V. After CO adsorption, the resonance level shifts out of the accessible bias range. The tip approaches the AuCO to compensate for the reduced LDOS and to maintain a constant electron current. The displacement of the 1.95-V state is consistent with a simple Blyholder picture, where electron charge is transferred from the CO 5σ orbital into unoccupied Au sp states [33]. The modified Au–CO hybrid state has a different energy, symmetry, and spatial localization and is unavailable as a final state for tunneling electrons. The presence of AuCO species on the surface was verified by inelastic electron tunneling (IET) spectroscopy

with the STM, detecting the AuCO hindered rotational mode at ± 35 mV [32].

A similar behavior was observed for CO adsorption onto Au chains on the NiAl surface [34, 35]. CO was either adsorbed onto pre-built chains or the chains were constructed around a single AuCO formed after gas exposure. The latter approach offers the opportunity to choose the CO position on the chain and was therefore preferred. The CO molecule is identified by a dip in the otherwise uniform chain height in STM topographies taken above 1.0 V (Fig. 5a). In images measured in the mV range, the CO appears as a small protrusion on the chain. In correspondence to the monomer case, the CO modifies the LDOS in the Au atom underneath the molecule, forcing the tip to lower the height. The spatial localization of the dip on the chain indicates that the CO preferentially interacts with a single chain atom and does not couple to the chain electronic system as an entity. The removal of the resonance level in the CO-affected Au atom prevents the hybridization with states in neighboring Au atoms. In analogy to a Pd impurity atom immersed in Au chains, adsorption of a CO molecule breaks the 1D electronic system into two independent parts. The chain sections on both sides of the AuCO show the electronic signature of isolated chains with an identical number of atoms.

The electronic properties of Au chains could be modified by pushing the CO along the chain axis using the STM tip (Fig. 5b). Whereas a bare Au₇ chain shows a low-energy dI/dV peak at 0.8 V, the state shifts to 0.85 V for Au₆(AuCO), 0.95 V for Au₄(AuCO)Au₂, and 1.1 V for Au₃(AuCO)Au₃. Conductance spectroscopy on the shorter part of the Au₄(AuCO)Au₂ chain reveals the double-peak structure of a Au dimer. The localization of the CO molecule on Au chains with different lengths was additionally identified in series of IET spectra taken along the chain axis [34]. The appearance of the hindered rotational mode of the AuCO at ± 37 mV along the chain perfectly matches the position of the dip in STM topographic images.

Adsorption of more than one CO molecule leads to a breakdown of the 1D electronic structure in atomic chains on NiAl(110). After heavy CO dosage, the uniform height of pure Au(PdAu)₅ chains transforms into an oscillating height pattern (Fig. 6). The two atomic species in the alloy chain become distinguishable again, whereby the five Pd atoms are imaged taller. The preferential CO binding to one atomic species leads

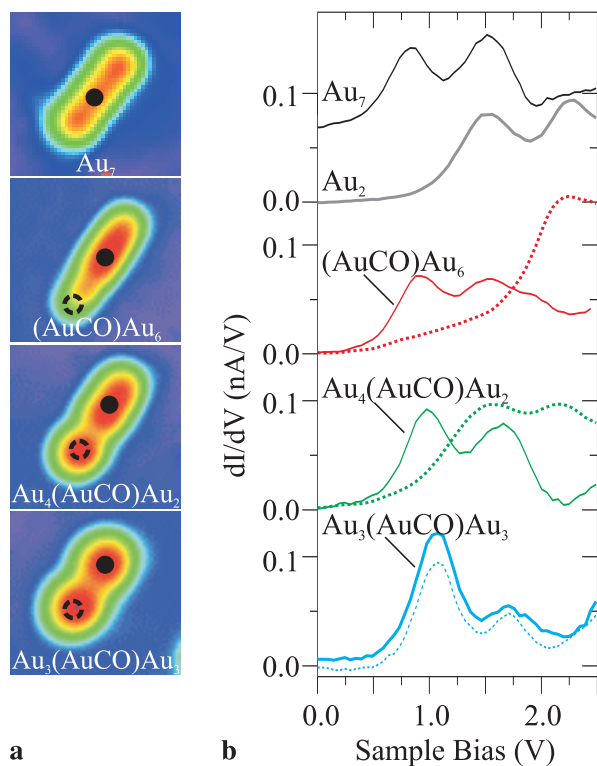


FIGURE 5 **a** STM topographic images and **b** dI/dV spectra of a Au₇ chain on NiAl(110) with a single CO molecule adsorbed at different positions. The CO location can be deduced from the dip in the chain height in the topographic images. Tip positions for dI/dV spectroscopy are marked in (a), where solid circles correspond to solid curves in (b) and broken circles are associated with the dashed spectra. The spectra demonstrate the disintegration of the 1D quantum well in Au₇ induced by the CO binding. For example, the spectrum taken over the Au₂ section of Au₄(AuCO)Au₂ (second dashed curve from the bottom) shows the double-peak structure of the isolated Au dimer (second solid curve from the top)

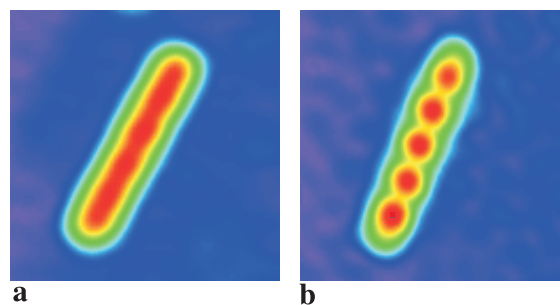


FIGURE 6 STM topographic image of a Au(PdAu)₅ chain on NiAl(110) **a** before and **b** after heavy CO dosage. The tunneling gap was set with $V_{\text{sample}} = 1.75$ V and $I = 1.0$ nA. Quantum-well states become localized due to the CO adsorption and Au and Pd atoms in the alloy chain can be distinguished

to a localization of the quantum-well states. The 1D electronic system develops into a series of single-atom quantum dots.

8 Conclusion

The experiments described in this paper demonstrate how atom manipulation with a STM tip can be exploited to manufacture aggregates from single atoms with unmatched precision. The technique was used to construct atomic chains on a NiAl(110) surface with different lengths, lattice constants, and elemental compositions. The electronic structure of the chains is dominated by a one-dimensional, free-electron-like band. Controlled changes in the band structure were initiated by modifications of geometric and chemical properties of the atomic chains. A substitution of the Au chain atoms for Pd atoms results in a shift of the band onset from 0.75 to 1.51 V. An increase of the lattice spacing enhances the effective electron mass of the band. The introduction of local impurities into atomic chains triggers a localization of the quantum-well states and leads to the formation of confined defect levels. The experimental approach opens new insights into the interrelation between topographic, chemical, and electronic properties of matter on the nanometer scale.

ACKNOWLEDGEMENTS The experiments were supported by the National Science Foundation, Grant No. 0102881. N. Nilius gratefully acknowledges the Deutsche Forschungsgemeinschaft for a fellowship. The authors thank M. Persson for many stimulating discussions.

REFERENCES

- 1 T.W. Odom, J.L. Huang, P. Kim, C. Lieber: *Nature* **391**, 62 (1998)
- 2 D.J. Hornbaker, S.J. Kahng, S. Misra, B.W. Smith, A.T. Johnson, E.J. Mele, D.E. Luzzi, A. Yazdani: *Science* **295**, 828 (2002)
- 3 B. Pampuch, O. Rader, T. Kachel, W. Gudat, C. Carbone, R. Kläsches, G. Bihlmayer, S. Blügel, W. Eberhardt: *Phys. Rev. Lett.* **85**, 2561 (2000)
- 4 N.F. Mott: *Metal-Insulator Transitions* (Taylor & Francis, London 1974)
- 5 J. Voit: *Rep. Prog. Phys.* **58**, 977 (1995)
- 6 K.H. Lau, W. Kohn: *Surf. Sci.* **75**, 69 (1978)
- 7 P.G. Collins, K. Bradley, M. Ishigami, A. Zettl: *Science* **287**, 1801 (2000)
- 8 F. Favier, E.C. Walter, M.P. Zach, T. Benter, R.M. Penner: *Science* **293**, 2227 (2001)
- 9 K. Kuhnke, K. Kern: *J. Phys.: Condens. Matter* **15**, 3311 (2003)
- 10 A. Mugarza, A. Mascaraque, V. Perez-Dieste, V. Repain, S. Rousset, F.J. Garcia de Abajo, J.E. Ortega: *Phys. Rev. Lett.* **87**, 107601 (2001)
- 11 P.W. Murray, I. Brookes, S.A. Haycock, G. Thornton: *Phys. Rev. Lett.* **80**, 988 (1988)
- 12 K. Kern, H. Niehus, A. Schatz, P. Zeppenfeld, J. George, G. Comsa: *Phys. Rev. Lett.* **67**, 855 (1991)
- 13 L. Pleth Nielsen, F. Besenbacher, I. Stensgaard, E. Lægsgaard, C. Engdahl, P. Stoltze, J.K. Nørskov: *Phys. Rev. Lett.* **74**, 1159 (1995)
- 14 K.N. Altmann, J.N. Crain, A. Kirakosian, J.L. Lin, D. Petrovykh, F.J. Himpsel, R. Losio: *Phys. Rev. B* **64**, 035406 (2001)
- 15 A. Kirakosian, J.L. McChesney, R. Bennewitz, J.N. Crain, J.L. Lin, F.J. Himpsel: *Surf. Sci.* **498**, 109 (2002)
- 16 D.M. Eigler, E.K. Schweizer: *Nature* **344**, 524 (1990)
- 17 L. Bartels, G. Meyer, K.H. Rieder: *Phys. Rev. Lett.* **79**, 697 (1997)
- 18 S. Fölsch, P. Hyldgaard, R. Koch, K.H. Ploog: *Phys. Rev. Lett.* **92**, 056803 (2004)
- 19 M.F. Crommie, C.P. Lutz, D.M. Eigler: *Nature* **363**, 524 (1993)
- 20 T. Jamneala, V. Madhavan, M.F. Crommie: *Phys. Rev. Lett.* **87**, 256804 (2001)
- 21 H.J. Lee, W. Ho: *Science* **286**, 5445 (1999)
- 22 B.C. Stipe, M.A. Rezaei, W. Ho: *Rev. Sci. Instrum.* **70**, 137 (1999)
- 23 N. Nilius, T.M. Wallis, W. Ho: *Science* **297**, 1853 (2002)
- 24 N. Nilius, T.M. Wallis, M. Persson, W. Ho: *Phys. Rev. Lett.* **90**, 196103 (2003)
- 25 The eigenstates E_n in a 1D quantum well with infinite walls are calculated from the effective electron mass m_{eff} , the well length L , and the quantum number n using $E_n = (\hbar^2/2m_{\text{eff}})(n\pi/L)^2$
- 26 T.M. Wallis, N. Nilius, W. Ho: *Phys. Rev. Lett.* **89**, 236802 (2002)
- 27 G. Mills, B. Wang, W. Ho, H.J. Metiu: *J. Chem. Phys.* **120**, 1138 (2004)
- 28 C. Kittel: *Introduction to Solid State Physics* (Wiley, New York 1996)
- 29 N. Nilius, T.M. Wallis, M. Persson, W. Ho: to be published
- 30 T.M. Wallis, N. Nilius, W. Ho: *J. Chem. Phys.* (2004), in press
- 31 N. Nilius, T.M. Wallis, W. Ho: *Phys. Chem. B* **108**, 14616 (2004)
- 32 T.M. Wallis, N. Nilius, W. Ho: *J. Chem. Phys.* **119**, 2296 (2003)
- 33 G. Blyholder: *J. Phys. Chem.* **68**, 2772 (1964)
- 34 N. Nilius, T.M. Wallis, W. Ho: *Phys. Rev. Lett.* **90**, 186102 (2003)
- 35 N. Nilius, T.M. Wallis, W. Ho: *Jpn. J. Appl. Phys.* **42**, 4790 (2003)